

Complex patterns of spontaneous initiation and termination of reentrant circulation in a loop of cardiac tissue

H. Sedaghat^{1†}, M.A. Wood², J.W. Cain¹, C.K. Cheng³
C.M. Baumgarten⁴, D.M. Chan¹

¹Department of Mathematics and the Center for the Study of Biological Complexity;

²Department of Internal Medicine-Cardiology and the Pauley Heart Center;

³Department of Computer Science and the Center for the Study of Biological Complexity;

⁴Department of Physiology and the Pauley Heart Center;

Virginia Commonwealth University, Richmond, Virginia, 23284-2014, USA

Abstract

A two-component model is developed consisting of a discrete loop of cardiac cells that circulates action potentials as well as a pacing mechanism. Physiological properties of cells such as restitution of refractoriness and of conduction velocity are given via experimentally measured functions. The dynamics of circulating pulses and their interactions with the pacer are regulated by two threshold relations. Patterns of spontaneous initiations and terminations of reentry (SITR) generated by this system are studied through numerical simulations and analytical observations. These patterns can be regular or irregular; causes of irregularities are identified as the threshold bistability of reentrant circulation (T-bistability) and in some cases, also phase-resetting interactions with the pacer.

Keywords Reentry; Loop; pacer; Thresholds; Bistability; Difference equations

1 Introduction.

Ventricular arrhythmia is the leading cause of cardiac arrest and sudden death. Clinical observations and implantable cardioverter defibrillators have accumulated a substantial amount of data on the occurrences of ventricular arrhythmia in patients [1, 36, 37, 38, 52, 59-61]. Temporal patterns of initiations and terminations of ventricular arrhythmia tend to exhibit substantial variations across different time scales, and their occurrences do not correlate decisively with medication, exertion, stress, lifestyles and similar factors. Arrhythmia events are not random; they show circadian patterns [36, 60] and also tend to occur in clusters. However, the detection times between consecutive events and clusters are spread out over time [37, 52, 59], making it difficult to understand their causes and make predictions about their occurrences. Unlike the circadian patterns, these clusterings or their patterns of occurrences are not affected by the long-term administration of

⁰This research was supported in part by a grant from Medtronic, Inc.

^{0†}Corresponding author; Email: hsedagha@vcu.edu

antiarrhythmic drugs [59]. In spite of the abundant data in existence, the basis for non-circadian patterns is not well-understood.

Many factors, ranging from internal cardiac mechanisms to external chance events play significant roles in shaping the electrocardiogram (ECG) recordings and the implantable defibrillator data. Separating all of the possible contributions is a formidable task, but understanding the influences of various factors and the extent to which each plays a role may have important consequences for the diagnosis and treatment of tachyarrhythmias. A number of prior studies using special preparations of animal cell cultures establish that complex, spontaneously generated patterns may occur without some of the features peculiar to the heart (e.g. the 3-dimensional geometry or biological features such as valves, different tissue layers and types, etc) [3, 25, 35, 44]. These studies also indicate (both theoretically and experimentally) that causes external to the heart, whether random or deterministic, are not always necessary for the occurrence of irregular behavior. A different class of studies that involve interactive self-oscillatory sources also establish the capability of basic cardiac mechanisms to generate complex rhythms without considering the whole heart [23, 28, 43].

From these and similar studies it may be inferred that changes in the basic internal cardiac mechanisms can play a significant role in generating and sustaining arrhythmias. To clarify the role of these basic internal mechanisms at a fundamental level, in this paper we focus on the unidirectional reentrant circulation of action potentials in a loop of ventricular tissue. Because of their pervasiveness, relative simplicity and importance in clinical arrhythmogenesis reentrant loops have received a great deal of attention [4, 8, 11, 14-16, 20, 26, 30, 41, 44, 48-50, 55]. Studying spontaneous initiation and termination of reentry (SITR) patterns in the loop context is considerably simpler than in the whole heart and can offer potentially useful insights into the clinically observed patterns of arrhythmia. In the construction of a workable model, a certain level of abstraction bridges over physiological complexities that do not play a central role in the long-term evolution of temporal patterns.

In this paper we consider a model that combines the traditional discrete loop with a pacer to form an interactive system. Fundamental thresholds are dynamically integrated so they can either trigger reentry or inhibit it. Although a relatively simple mechanism, this composite system has two important features: It is an essential component of a well-known cardiac anomaly; and it is capable of generating complex initiation and termination patterns.

In a series of case-studies we show that the loop-pacer mechanism may be responsible for irregularities in onset and termination of reentry beyond such pervasive factors as tissue heterogeneity, the geometry of the heart and other physiological and non-physiological factors. Even without such complexities, the SITR patterns generated by the loop-pacer system can be complex; i.e. they contain many regular features yet their evolution over time is difficult to predict. We trace this complexity to the interaction of a threshold with bistability of the reentrant circulation and in some cases, also to the inherent discontinuity of phase resetting interactions between the loop and the pacer. Bistability is an inherent physiological characteristic that may be attributed to non-uniformities in the restitution of action potential duration (APD); this feature emerges prominently when conduction velocity (CV) is properly matched with APD. When this happens (e.g. when the

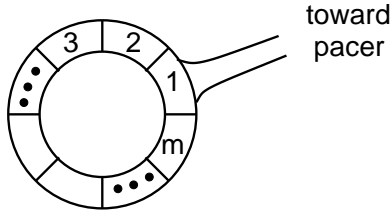


Figure 1: Schematic diagram of a loop joined to the rest of the heart by a single conducting pathway.

length of the loop is within a certain range) the SITR patterns become considerably more complex and unpredictable.

2 The threshold model.

In this section we describe the main features of the loop-pacer model, leaving a few additional details to Section 4. The pacemaker is a self-oscillatory mechanism that is tied to the reentrant circuit (the loop in this paper) via a time lag or delay parameter and a special threshold.

2.1 The loop.

Consider a loop of cardiac tissue consisting of cells that conduct action potentials and assume that a single conducting pathway connects the loop to the rest of the heart. Let the physical length of the loop be denoted by L measured in centimeters. Divide the loop into m sets or aggregates of cells, each of which may be called a *cell aggregate* or for brevity, just a “cell.” The cell aggregate that is connected to the only pathway out of the loop is also the gateway through which pulses enter the loop or exit it; we label it Cell 1; see Figure 1. This cell is adjacent not only to Cell 2, but also to Cell m at its other end.

For each integer i between 1 and m , label the length of the i -th Cell ΔL_i . These cell aggregates’ lengths are not necessarily equal but of course, they add up to L . Since each cell aggregate must have at least one cardiac cell in it, ΔL_i has a natural lower bound, namely the nominal length of a single cardiac cell (about 0.01 cm or 100 microns). The closer all ΔL_i are to this lower bound, the greater is the number m of cell aggregates in a loop of fixed length L ; for a 12 cm loop with cells of length 0.01 cm, the number of cells is 1200. While for discrete modeling it is not necessary to pick m that large, it needs to be large enough (hence each cell aggregate small enough) that the conduction velocity from one end of an aggregate to the other can be taken to be approximately constant. This assumption is essential if the restitution of conduction time (CT) is defined in terms of the restitution of CV, as we do later on.

We assume that all the cardiac cells within a given aggregate are identical. If all cells in the *entire loop* have identical physiological characteristics then we may also let cell aggregates all

have equal lengths. In such a case, the loop is said to be “homogeneous.” Otherwise the loop is “heterogeneous.”

To initiate unidirectional circulation, it is necessary that a unidirectional block (UB) exist somewhere in the loop; for simplicity, we place it in Cell 1, the gateway to the loop; see Figure 1. Thus Cell 1 is able to activate Cell 2 but not Cell m . For our simulations, we use a simplified version of the UB time window that is defined by a threshold value for the diastolic interval (DI). Thus conduction is blocked in any cell whose DI is not greater than the threshold DI^* ; see Section 4 below for more details. Such a minimum value is used in [26] as a termination mechanism for explaining the experimental results of [20]; also see [19].

2.2 Restitution functions.

We use the term “restitution” generally for relations that give a particular quantity, e.g. action potential duration or conduction time, as a function of the diastolic interval (DI). The DI (usually measured in milliseconds, ms) is the rest or recovery period for the cell which essentially starts with the end of the refractory period and ends when the cell is activated again.

2.2.1 APD restitution.

In its most basic form, the action potential duration or APD is the length of time (usually measured in milliseconds, ms) that a cell is active after excitation. For our purposes, we may think of APD as a cell’s effective refractory period (ERP) during which no excitations, even strong ones, can elicit new action potentials. The restitution of APD, which can be experimentally measured or derived from ionic models, is the most extensively studied of restitution relations [2, 4-8, 10, 11, 21, 24, 26, 29, 32, 33, 42, 45, 48, 50, 53-57]. Any APD restitution function, whether experimentally measured or analytically derived can be used in this model. For the numerical simulations in this paper, we use an APD restitution function that is fitted to the experimental data by Koller, et al [33] where APD values were recorded in two types of patients, those with and those without structural heart disease (SHD). The following is a possible fit to their averaged data displayed in Figure 1 in [33] for SHD patients:

$$A(DI) = a_1 - a_2 e^{-\sigma_1 DI} - a_3 e^{-\sigma_2 (DI - \tau_1)} - a_4 e^{-\sigma_3 (DI - \tau_2)^2} + \frac{a_5 (DI - \tau_3)}{(DI - \tau_3)^2 + a_6} \quad (1)$$

with parameter values

| a_1 | a_2 | a_3 | a_4 | a_5 | a_6 | σ_1 | σ_2 | σ_3 | τ_1 | τ_2 | τ_3 |
|-------|-------|-------|-------|-------|-------|------------|------------|------------|----------|----------|----------|
| 350 | 157 | 8 | 20 | 1700 | 1200 | 0.0021 | 0.025 | 0.0004 | 80 | 136 | 82 |

A graph of this function is shown in Figure 2. Expressing the APD as a function of DI in the above manner represents only a first order of approximation (see Section 4 below).

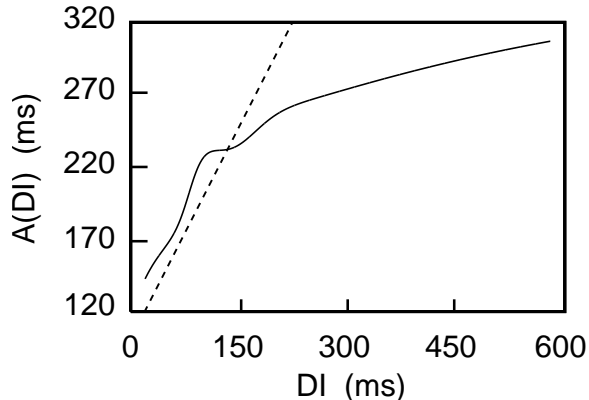


Figure 2: The APD restitution curve given by (1). The dashed line has slope 1 and is included for reference.

2.2.2 CT restitution.

Each cell conducts an action potential through it in a finite amount of time. This time interval, usually measured in milliseconds, is referred to as the conduction time (CT) [4, 26, 50]. Experimentally measured CT restitution functions are not as readily available for human hearts as the APD restitution functions; however, they may be readily derived from CV restitution functions through the relation

$$C(DI) = \frac{\Delta L}{V(DI)} \quad (2)$$

where C and V are, respectively, the CT and the CV restitution functions. This derivation is valid if as mentioned earlier, V is essentially constant over the length of each cell (or cell aggregate) and thus no spatial dependence is required in V .

For discussions of CV restitution functions see [2, 7, 8, 11, 12, 14-16, 20, 22, 53, 54, 56]. For our simulations we use the following expression

$$C(DI) = \frac{\Delta L}{c} [1 + de^{-\omega DI}], \quad DI > 0 \quad (3)$$

with parameter values:

| ΔL | c | d | ω |
|------------|------------|-----|-----------------------|
| 0.1 cm | 0.07 cm/ms | 1 | 0.02 ms ⁻¹ |

These numbers are obtained using (2) and a reasonable fit to the human-rescaled, guinea pig data for CV from [22, 54]. The value of ΔL corresponds to 10 nominal cells. The number c in (3) is the maximum CV; in more common (though less uniform) units, the fitted number in the above table would be 0.7 m/s. By changing the parameters in (3) we may achieve conduction slow-downs in different ways, as shown in Figure 3.

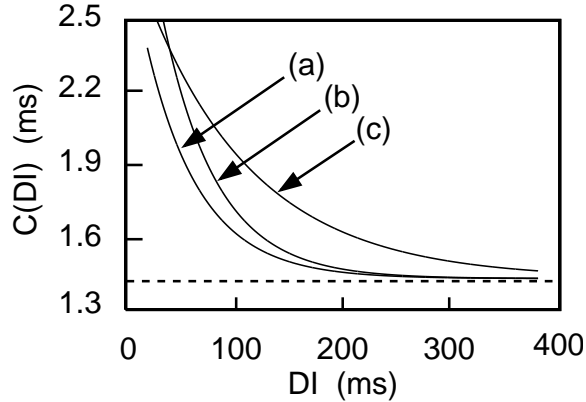


Figure 3: CT restitution curves given by (3) for several choices of parameters. For each curve, $\Delta L = 0.1$ and $c = 0.07$. (a) $d = 1$ and $\omega = 0.02$; (b) $d = 1.5$ and $\omega = 0.02$; and (c) $d = 1$ and $\omega = 0.01$.

2.3 The two rhythms.

In the absence of reentry, a pacer (the sinus node or an ectopic focus) drives the ventricular contraction cycle. If reentry is initiated and interrupted then the pacer and the loop fall out of phase and it is necessary to carefully model their interaction. For this purpose we define two rhythms or clocks: The pacer's rhythm which has a prescribed beat pattern (fixed or variable) and the system's rhythm which is reset when reentry is initiated or terminated. These two rhythms are related via a pacer threshold (seen the next section) and a delay term that we now define.

The *time of occurrence* for the n -th beat (following a fixed reference beat) can be tracked and calculated using the following quantity, namely, the sum of usually variable cycle lengths (after a DI adjustment):

$$\rho_n = \sum_{j=1}^n CL_j + (DI_{1,0} - DI_{1,n}), \quad CL_j = A(DI_{1,j-1}) + DI_{1,j}.$$

Let the time of occurrence of the k -th pacer beat be denoted by β_k (starting from the same reference point in time as that for ρ_n). The difference

$$\beta_k - \beta_{k-1} = B(k)$$

is the duration of each such beat. In our simulations $B(k)$ is defined arbitrarily in order to facilitate our study of the SITR patterns. If the pacer is the sinus node then $B(k)$ is influenced by a variety of deterministic and stochastic factors, such as circadian, weekly and seasonal variations, lifestyles, drugs, the autonomic system and so on. Thus a single, all purpose formula for $B(k)$ does not exist.

The two rhythms ρ_n and β_k fall out of phase if reentry occurs as noted earlier. To model their interaction, we define the *first* pacer pulse that reaches Cell 1 in beat n as the *least* integer k_n such that

$$\beta_{k_n} > \rho_n + \delta_n. \quad (4)$$

The variable delay term δ_n here represents a *time lag* that results from the blocking of the pacer by the retrograde reentrant wave propagating toward the pacer. A number of things may affect δ_n ; these include the different types of tissue in which pulses propagate (retrograde and antegrade), the electrotonic spread of current in conducting tissue between the pacer and the loop, and the effect of reentrant waves on the pacer's intrinsic beat rate. For simplicity we do not consider the electrotonic currents and tissue heterogeneity. We assume also that the pacer itself is protected in the sense that its intrinsic beat rate is not affected by the reentrant activity.

Therefore, we use a simple definition for δ_n as follows:

$$\delta_n = \begin{cases} \delta, & \text{if pulse } n-1 \text{ was reentrant} \\ DI^*, & \text{otherwise} \end{cases}, \quad \delta > DI^*.$$

If the loop is not in reentry, then δ_n may take the minimum value DI^* since Cell 1 must have at least that much rest time after its ERP before it can be reactivated. High frequency reentrant waves typically disassociate a slow pacer such as the sinus node. This situation is modeled here by choosing a sufficiently large value of the delay parameter δ so as to inhibit the pacer from interfering with the reentrant circulation. Small values for δ , which promote pacer interference, may be feasible in certain circumstances, e.g. when there are pathways from the pacer's site to the site of the loop that are protected from the fast reentrant waves by pathologies.

To determine the index value k_n we may generate the sequence β_k independently of ρ_n and for each n mark the values k_n that satisfy (4). This process is carried out internally during each simulation run; an analytical relationship is generally not easy to find. However, if $B(k) = B_0$ is constant then such a relationship is easy to find; in this case we have $\beta_{k_n} = k_n B_0$ with

$$k_n = \left\lceil \frac{\rho_n + \delta_n}{B_0} \right\rceil$$

i.e., the least integer that is greater than or equal to the ratio $(\rho_n + \delta_n)/B_0$. This simple relationship makes explicit the discontinuity that results from phase resetting in our model.

2.4 Modes and thresholds.

We distinguish between two primary dynamic modes for the loop-pacer system: The *reentry mode* where an action potential circulates in the loop by itself and the *paced mode* where the action potential in the loop comes from the pacer. The system's mode in each beat changes on the basis of threshold relations to be defined below. The modes are defined by systems of partial difference equations that track the circulating pulse in both space and time. Introductory material

on ordinary and partial difference equations can be found in [9, 17, 31, 40, 51]. Technically, the dynamical system consisting of the loop, the pacer and the associated thresholds is a polymodal structure in the sense of [51].

2.4.1 Dynamic activation duration.

Let $DI_{i,n}$ be the DI of Cell i in beat n . Define the *firing indicator* function as

$$\begin{aligned} \phi_{1,n} &= 1, \quad \text{and} \\ \phi_{i,n} &= \begin{cases} 1, & \text{if } DI_{i,n-1} > DI^* \text{ and } \phi_{i-1,n} = 1 \\ 0, & \text{if } DI_{i,n-1} \leq DI^* \text{ or } \phi_{i-1,n} = 0 \end{cases}, \quad i = 2, \dots, m. \end{aligned}$$

This quantity specifies conditions under which the i -th cell fires an action potential in beat n ; these conditions simply require that (a) the preceding Cell $i - 1$ fired and (b) the DI of Cell i in the preceding beat $n - 1$ exceeded the minimum value DI^* as is required for propagation.

We assume that Cell 1 fires in every beat whether by a reentrant pulse or by a pulse from the pacer.

Let $APD_{i,n}$ denote the action potential duration of Cell i in beat n so that if the i -th cell does not fire in beat n then $APD_{i,n} = 0$ (otherwise, $APD_{i,n} = A_i(DI_{i,n-1})$). The dynamic *activation duration* is defined as

$$AD_{i,n} = \phi_{i,n} A_i(DI_{i,n-1}), \quad i = 1, 2, \dots, m$$

where A_i is the APD restitution function for Cell i . Note that $AD_{1,n} = APD_{1,n} = A_1(DI_{1,n-1})$ for Cell 1 in every beat. In the following sections (except in Case-study 4) we assume that the loop is APD homogeneous so that $A_i = A$ for all $i = 1, 2, \dots, m$ where A is given by (1).

2.4.2 Paced mode.

In this mode the pacer determines the DI values $DI_{i,n}$ rather than a reentrant pulse in the primary loop; the circulation is assumed unidirectional owing to an active UB. We use the following system of m equations:

$$DI_{1,n} = \beta_{k_n} - \rho_n \tag{5a}$$

$$\begin{aligned} DI_{i,n} &= DI_{i-1,n} + AD_{i-1,n} - AD_{i,n} + CT_{i-1,n+1} - CT_{i-1,n} \\ &\quad + (1 - \phi_{i,n})DI_{i,n-1} - (1 - \phi_{i-1,n})DI_{i-1,n-1} \end{aligned} \tag{5b}$$

with $i = 2, \dots, m$.

Here C_i is the CT restitution function for Cell i . The above system of equations determines the DI values using the first pacer beat after time instance ρ_n (beat n in progress). Figure 4 illustrates equations (5b) and (6b). The first five terms in (5b) simply express in mathematical terms what

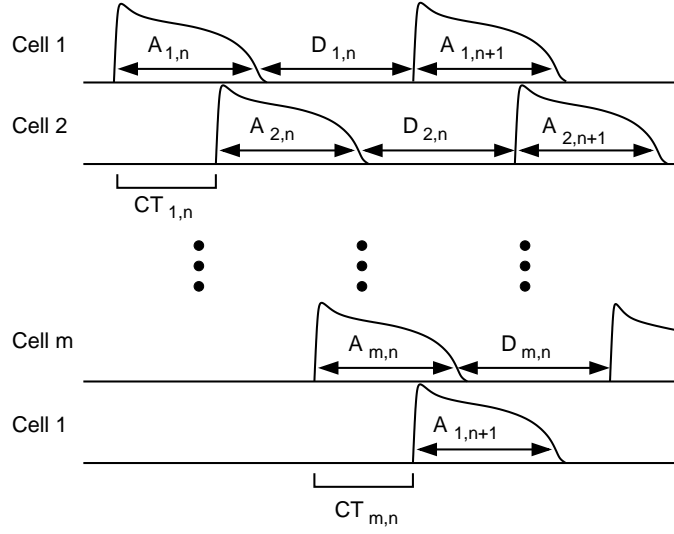


Figure 4: Schematic diagram of a circulating action potential in a ring of m cells; A is APD, D is DI and CT is the conduction time. The sizes of A, DI and CT are selected arbitrarily for clarity of illustration.

we might state less precisely using the English language. They are the same for tissue fibers as they are for loops; see, e.g. [68]. The last two terms in the definition of $DI_{i,n}$ in (5b) allow for proper adjustment of the DI value (without double counting) when Cell i does not fire in beat n (see comments on the reentry mode below). In typical loop models in prior literature all cells fire so these two terms would drop out.

2.4.3 Reentry mode.

In this mode the reentrant loop drives the ventricles ectopically. Thus $DI_{1,n}$ is the difference between the APD of Cell 1 and the total conduction time for unidirectional circulation once around the ring, i.e.

$$DI_{1,n} = \sum_{j=1}^m CT_{j,n} - A_1(DI_{1,n-1}) \quad (6a)$$

$$DI_{i,n} = DI_{i-1,n} + AD_{i-1,n} - AD_{i,n} + CT_{i-1,n+1} - CT_{i-1,n} \quad (6b)$$

$$+ (1 - \phi_{i,n})DI_{i,n-1} - (1 - \phi_{i-1,n})DI_{i-1,n-1}$$

with $i = 2, \dots, m$.

It is not hard to show that the system of m equations (6) is equivalent to the coupled map

lattice equations in [51] when $\phi_{i,n} = 1$ for all i and n .

Equations (6) are not valid if some of the DI values fall below the threshold DI^* or if a stray pacer pulse gets into the loop (i.e. if the right hand side of (6a) exceeds the right hand side of (5a)). The following threshold relations ensure a consistent scenario.

TC: The *circulation threshold* (or *head-tail* or *conduction block threshold*) is based on the following set of inequalities:

$$\sum_{j=1}^m CT_{j,n} - A_1(DI_{1,n-1}) > DI^*,$$

$$DI_{i-1,n} + AD_{i-1,n} - AD_{i,n} + CT_{i-1,n+1} - CT_{i-1,n} > DI^* \quad \text{for } i = 2, \dots, m.$$

They ensure that the DI values $DI_{i,n}$ in Equations (6) exceed DI^* , as is necessary for the generation of action potentials. If any of the above inequalities fails in a Cell i then a wavefront reaches its own tail in that particular cell and circulation stops until the arrival of the next pacer pulse. In this case we say that TC fails in Cell i .

TP: The *pacer threshold* (or *phase resetting threshold*) is defined by the following inequality:

$$\sum_{j=1}^m CT_{j,n} - A_1(DI_{1,n-1}) < \beta_{k_n} - \rho_n.$$

This inequality ensures that the reentrant pulse (rather than a stray one from the pacer) reactivates Cell 1.

Mode switching criteria. Equations (6) are used if TP holds and also TC holds in Cell 1. If for some Cell $i \geq 2$ TC fails, then (6b) can still be used to find the DI values for beat n , but we switch to equations (5) for beat $n + 1$. If TC fails for $i = 1$, or if TP fails then we use (5) for beat n .

2.4.4 Bidirectional circulation (BDC) mode.

In the absence of unidirectional block the pacer sends two pulses in the loop with Cell 1 activating both Cell 2 and Cell m . These pulses propagate in opposite directions to eventually annihilate each other in some cell in the loop. Transitions into and out of this bidirectional circulation mode are governed by TC, TP and a UB threshold (TUB); see Section 4 below. We assume for simplicity that TUB never fails so that the BDC mode need not be discussed in this paper.

3 SITR patterns.

In this section we present the results of numerical simulations of our threshold model along with some analytical observations. Due to the large number of different types of behavior that can occur by changing one or more of the many variables involved, providing a comprehensive list of essentially different patterns is not feasible here. We therefore present our main results in the form of a few model case-studies and for additional results we refer the interested reader to our web site: www.people.vcu.edu/~hsedagha/SITR.

Each case-study below consists of one or more “runs,” i.e. sets of iterations of the propagation equations. Each run is based on a fixed set of parameter values and we call each iteration in a given run a “beat”. For each run we need to specify m initial DI values $DI_{i,0}$. This specification of DI values is a technical representation of the occurrence of a premature stimulation in our model.

Computational accuracy is not a major issue in the qualitative studies in this paper. However, calculating the values of the various nonlinear functions (e.g. the exponentials in the APD and CV restitution functions) generate round-off errors that can accumulate in certain cases (e.g. runs in Case-study 4). Therefore, results obtained by different programs, codes or levels of precision (single or double) may be different from some of those that we have presented, although the qualitative features are usually retained.

3.1 Mode sequences.

The following conventions facilitate the presentation of results in this section:

For a loop consisting of m cells if a reentrant pulse is blocked at Cell j in a particular beat, then we define the *reentry value* of that beat as the ratio $(j - 1)/m$; this ratio will be abbreviated as $[j]$.

If a reentrant pulse completes a turn around the loop then the reentry value is 1.

If a reentrant pulse is blocked in Cell j after t complete turns around the loop then the reentry value is $t[j]$.

If a beat occurs in the paced mode (i.e. one of the thresholds TC or TP fails) then we assign it the value -1 . Thus t consecutive paced beats appear as $-t$.

If the pattern is locked in the reentry mode, we use the symbol ∞ ; if it is locked in the paced mode, we use $-\infty$.

Adding up consecutive reentry mode beats and consecutive paced mode beats gives a sequence of numbers consisting of integers whose sign tell us the mode of system in various sets of beats. Examples of mode sequences and more details on them are found in the case-studies below.

3.2 Bistability and thresholds.

We call the loop-pacer system *bistable* if there are two or more coexisting stable DI configurations or state vectors, each of which can be reached from a particular region of the m -dimensional state space. If there are more than two distinct, coexisting stable states then the system is *multistable*.

Bistability may be attributed to the non-concavity of the APD restitution function [50]. The APD function (1) whose graph has bumps and twists is also non-concave. Proper CT restitution parameters are required to realize bistability; i.e. the CT and APD restitution parameters must be properly matched. Because the length L of the loop affects the conduction time through it, bistability may emerge or fade as L is changed with other CT parameters fixed [50].

A bistable regime can affect SITR patterns by causing the violation of the circulation threshold TC without any changes in the APD or CT parameters, or any changes in the pacing rate. This situation occurs if the bistable regime satisfies the following *threshold bistability* condition:

T-bistability: There are two distinct stable states in the reentry mode: In one state the DI values cross DI^* and cause the failure of the circulation threshold TC at some cell within the loop, but in the other state the DI values are always greater than DI^* .

An example of T-bistability is shown in Figure 7 below; other examples of T-bistability occur in the next section (Case-study 1). The m -dimensional state space of a T-bistable system is partitioned into two regions or basins of attraction. As a SITR pattern evolves with the motion of the DI state vector, mode changes occur if the state vector crosses over into the basin of attraction of a different stable regime.

3.3 Case-study 1: T-bistable reentry.

In this section we establish that T-bistability lends a measure of unpredictability to SITR patterns that is not due to phase resetting disruptions by the pacer (i.e. TP failures). For instance, comparing the mode sequences in Runs 1.2, 1.4 and 1.6 below we see that the initial few bursts of fast, reentrant beats provide no obvious clues about the eventual modes that the patterns lock into.

Consider a homogeneous loop with the APD and CT restitutions given by (1) and (3). We also set the length L and other parameters as:

| L | m | DI^* | δ | B_0 |
|---------|-----|---------|----------|--------|
| 12.5 cm | 125 | 15.3 ms | 120 ms | 320 ms |

where B_0 is the fixed cycle length of the pacer; it is chosen small in this case-study to facilitate re-initiations of reentry. The value of δ is set high enough to inhibit pacer interference (TP never fails). The following table summarizes the results of simulations; it is followed by a series of observations and elaborations.

| Run No. | $DI_{i,0}, i = 1, \dots, 125$ | SITR pattern mode sequence |
|---------|-------------------------------|---|
| 1.1 | 200 ms | $\{-2, 2, -2, 2, \dots\}$ |
| 1.2 | 100 ms | $\{-2, 4, -2, 32[73], -2, \infty\}$ |
| 1.3 | 80 ms | $\{-1, \infty\}$ |
| 1.4 | 70 ms | $\{4, -2, 14, -2, 4, -2, 22[49], -\infty\}$ |
| 1.5 | 60 ms | $\{\infty\}$ |
| 1.6 | 50 ms | $\{11, -2, 4, -2, 27[57], -2, \infty\}$ |

(i) In Run 1.1 the SITR pattern immediately locks into a regular form of 2 paced beats followed by 2 reentrant beats. In Runs 1.2, 1.3, 1.5 and 1.6 the SITR pattern locks into the reentry mode. In Run 1.4 the paced mode is locked into. Note that the only thing that is changing from one run to the next is the initial DI values.

(ii) In Runs 1.2, 1.3, 1.5 and 1.6 the DI values in the sustained or locked reentry modes converge to a fixed number and the eventual values of the fundamental parameters are

| DI | APD | cycle length CL = APD+DI |
|---------|----------|--------------------------|
| 59.4 ms | 173.6 ms | 233 ms |

The fixed, limiting DI value 59.4 represents a stable *convergent state*. This equilibrium DI is locally stable (attracting) because using the restitution functions (1) and (3) we compute [4, 26]

$$A'(59.4) + C'(59.4) = 0.90 < 1.$$

(iii) In Runs 1.2, 1.4 and 1.6 all the spontaneously terminated reentry bursts have oscillating (quasiperiodic) DI. Thus APD and CL also oscillate similarly. The oscillatory state is stable and eventually crosses $DI^* = 15.3$ ms. Hence there is T-bistability (the oscillatory one and the convergent one) which is responsible for mode changes in each run.

For example, in Run 1.2 the 2nd initiation of reentry (the 32-beat burst) starts with the DI state-vector in the basin of attraction of an oscillatory state which expands enough for the DI values to cross DI^* (TC fails); see Figure 5. This terminates the second reentry burst at Cell 73 in the 41st beat. This is the same type of termination mechanism as that in [19, 20, 26]; this type of oscillations in DI are also seen in [56] where they are related to the T wave alternans in ECG recordings; also see [35] in this regard. With the 3rd initiation of reentry, the DI state-vector falls in the basin of attraction of the convergent state which then effectively “traps” the DI trajectory and locks the SITR pattern into the reentry mode (here then, simplicity of behavior is not a good thing).

(iv) Examination of the simulation data for Run 1.4 shows a recurrent failing of TC in Cell 1 after the last burst of 23 reentrant beats. For all sufficiently large values of n ,

| $DI_{1,n}$ | $APD_{1,n}$ | CL_n |
|------------|-------------|--------|
| 96.6 | 223.4 | 320 |

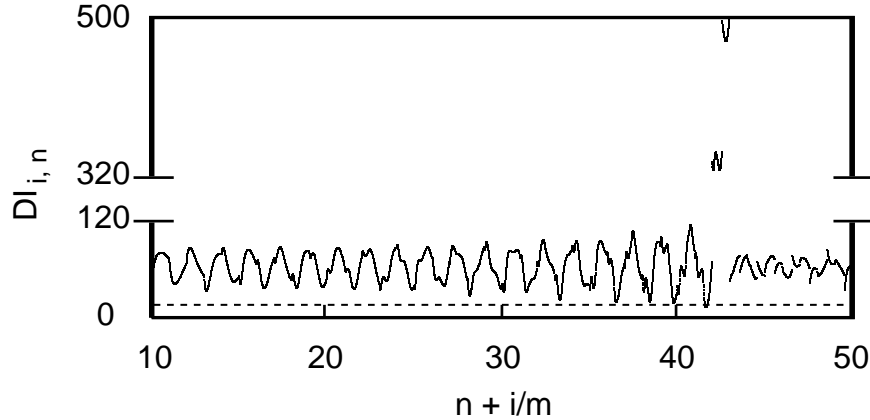


Figure 5: Results of Run 1.2, showing variation of DI in Beats 10 through 50. The dashed line corresponds to $DI^* = 15.3$. Amplification of oscillations in DI leads to termination of reentry in Beat 41, Cell 73 because $DI_{73,41} < DI^*$. With Beat 44 reentry is re-initiated and the system locks into the stable convergent state (after some transient oscillations).

The number 96.6 is the equilibrium DI for the paced mode with pacing period $B_0 = 320$. The paced-mode equilibrium happens to be stable because in the absence of reentry the paced mode is governed by the one-dimensional difference equation

$$DI_{1,n} = F(DI_{1,n-1}) = B_0 - A(DI_{1,n-1})$$

with $F'(96.6) = -A'(96.6) = -0.901$; i.e. $|F'(96.6)| < 1$. Why the transition to the stable paced equilibrium occurs in this run and not others is unclear. Figure 6 shows the changes in DI values in this run.

(iv) In Run 1.5, the given initial DI values put the state vector in the basin of attraction of the convergent state of the system. This is evidently not the case in Run 1.6 with even shorter DI. In Run 1.6, as in Run 1.4, the initial mode is oscillating-DI reentry.

3.4 Case-study 2: Non-T-bistable reentry.

We now consider some longer loops than in Case-study 1 for comparison. In these loops bistability is present but does not satisfy the T-bistability condition. A smaller variety of different SITR patterns are obtained (with all other system parameters having the same values as in Case-study 1). We consider two different lengths:

$L = 13$ cm ($m = 130$) where stable oscillating states exist all of which fail TC, but the convergent mode is absent since the DI fixed point of about 62.5 ms is unstable [4, 26]

$$A'(62.5) + C'(62.5) = 1.013 > 1.$$

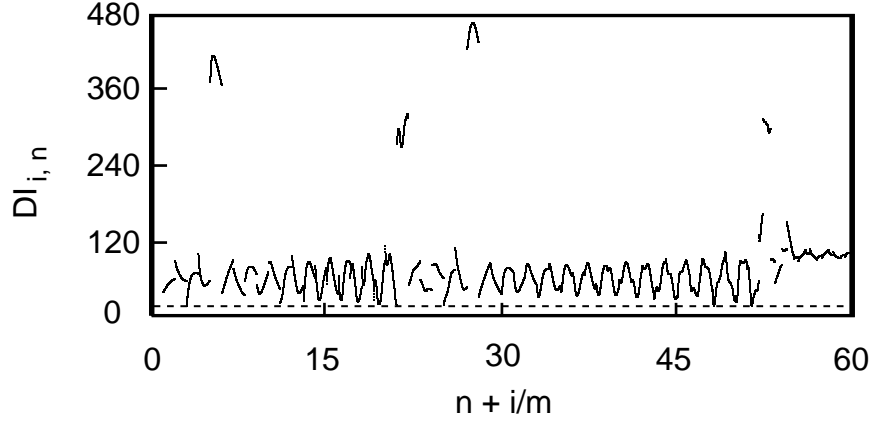


Figure 6: Results of Run 1.4, showing variation of DI in Beats 1 through 60. The dashed line corresponds to $DI^* = 15.3$. The four interruptions of reentry due to conduction block (TC fails) are seen as brief jumps to high DI. The last interruption terminates reentry and locks the system in the paced mode.

$L = 14$ cm ($m = 140$) where all of the stable oscillating states (there is at least one) satisfy TC. The convergent mode is again absent for the same reason as above:

$$A'(68) + C'(68) = 1.253 > 1.$$

To save space let us abbreviate repetitions or locked mode patterns with bars:

$$\overline{k, -j} = k, -j, k, -j, \dots \quad (7)$$

The following table summarizes the results of simulations; it is followed by a series of observations and elaborations.

| Run No. | $DI_{i,0}$ | $L = 13$ cm | $L = 14$ cm |
|---------|------------|--|---------------------------------|
| 2.1 | 200 ms | $\overline{-2, 2}$ | $\{-2, 2, -2, \infty\}$ |
| 2.2 | 100 ms | $\{-2, 4, -2, 12[60], -2, 2\}$ | $\{-2, \infty\}$ |
| 2.3 | 80 ms | $\overline{2, -2}$ | $\{-1, 1, -2, 2, -2, \infty\}$ |
| 2.4 | 70 ms | $\{12, -2, 10[79], -2, 17[79], \overline{-2, 5[79]}\}$ | $\{12, -2, 2, -2, \infty\}$ |
| 2.5 | 60 ms | $\{56, \overline{-2, 2}\}$ | $\{-1, 10, -2, 9, -2, \infty\}$ |
| 2.6 | 50 ms | $\{3, -2, 4, -2, 12[60], -2, 2\}$ | $\{-\infty\}$ |

(i) The SITR patterns for the 14 cm loop are expected to lock into the reentry mode since the stable states do not fail TC to cause terminations. The exception is Run 2.6 where possibly owing to the greater length of the loop, a pulse from the pacer has time to activate Cell 1 and block the

premature simulation from reentering the loop (threshold TP fails). It is not clear why reentry does not re-initiate as in Run 2.5.

(ii) In the case of the 13 cm loop the repeated terminations can be attributed to the fact that the stable states all fail TC; thus the patterns cannot lock into the reentry mode.

(iii) For both of these loops, the eventual form of the SITR pattern is more predictable than the T-bistable loop of Case-study 1. On the other hand, the transient bursts of fast beats still seem difficult to predict.

3.5 Case-study 3: Special patterns.

Run 3.1 (*more T-bistability*). This run presents a complex SITR pattern that locks into a long cycle of several initiations and terminations. Make the following changes to parameters in Run 1.2:

| | |
|-----|--------|
| d | B_0 |
| 1.3 | 315 ms |

Note that the increase in d from 1 to 1.3 in this run causes a slight elevation of the CT restitution curve (i.e., a conduction slow-down) at low DI values; see Figure 3.

(i) In this run, after a transient period of spontaneous initiations and terminations, a long 62-beat pattern emerges that is repeated; i.e. the SITR pattern locks into a 62-beat cycle containing several bursts of fast reentrant beats. The mode sequence for this run is as follows, with the pattern between starred numbers repeating:

$$\{-2, 8[81], -1, [35], -2, 4, -2, 7[24], -1, [18], -2, 8[18], * -1, [12], -2, 7[12], -1, [12], -2, 10[49], -2, 5[49], -2, 4, -2, 7[22], -1, [19], -2, 7[19], * -1, [12], -2, 7[12], -1, [12], -2, \dots\}$$

(ii) The DI equilibrium of approximately 64 ms is unstable in this run since

$$A'(64) + C'(64) = 1.073 > 1.$$

This instability is caused by the greater value of d and results in the absence of the convergent state. Nevertheless, there is T-bistability where one of the stable oscillating states does not fail TC but another oscillating state does. In the first oscillatory state, DI values come very close to DI^* ; see Figure 7. This proximity increases the sensitivity to transient effects of mode changes and makes locking into the reentry mode an improbable event.

Run 3.2 (*pacemaker action*). In Case-studies 1 and 2 we see that the convergent reentry pattern is “sticky” i.e. once this pattern is attained, reentry does not self-terminate by the circulation mechanism in the loop. However, pacemaker interaction with the loop can lead to termination in some cases by changing the convergent pattern to a terminating oscillatory one in a T-bistable case.

All parameters are as in Run 1.5 (hence there is T-bistability) except that now:

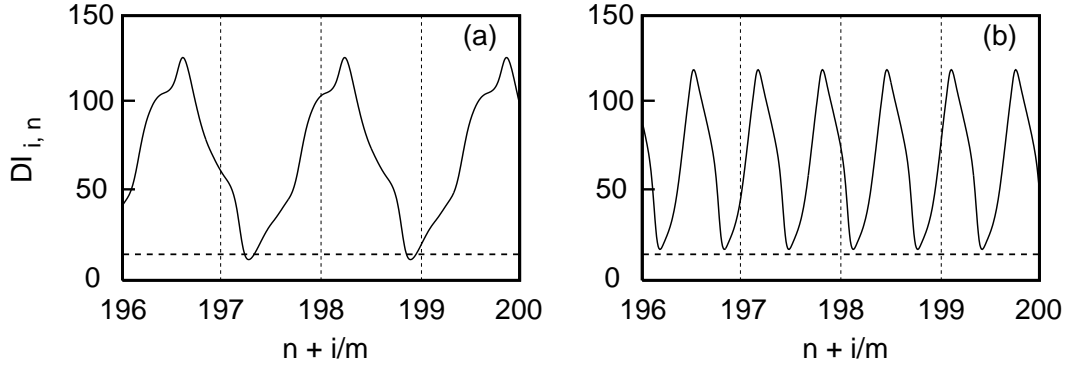


Figure 7: Two distinct stable states illustrating T-bistability in Run 3.1. (a) If $DI_{i,0} = 67$ for all i , the graph crosses the dashed horizontal line $DI = 15.3$; for the sake of illustrating the quasiperiodic nature of oscillations in reentry mode, the graph ignores TC since reentry would terminate with the first such crossing. (b) $DI_{i,0} = 66$ for all i . Reentry is sustained with quasi-periodic variation of DI.

| | |
|----------|--------|
| δ | B_0 |
| 45 ms | 800 ms |

We have set the pacing period at the nominal sinus length to eliminate the effects of fast pacing. The smaller value of δ promotes interference by the pacer.

(i) The mode sequence for this run, which may be compared with Run 1.5, is:

$$\{40, -1, 15, -\infty\}.$$

(ii) Reentry is initiated with Beat 1 by a premature stimulation, and the DI values begin to approach the limiting value 59.4 ms as in Run 1.5. However, TP fails in Beat 41; a stray pulse from the pacer enters the loop and changes the reentry DI pattern from the convergent type to an oscillating one; see Figure 8. The quantities PL_n , $PDI_{1,n}$ in Figure 8 are the right hand sides of equations (5a) and (6a), respectively.

The oscillating DI pattern crosses the DI^* threshold (TC fails) in Beat 55 and reentry terminates in this beat.

3.6 Case-study 4: Slow pacing, heterogeneity and PVC's.

When the pacing period is long (say, within the nominal sinus range of 800 ± 350 ms) and the loop is homogeneous, *re-initiations* of reentry do not occur with the above CT and APD parameters in the absence of premature stimulations or ectopic sources. The low CT (or high CV) in the loop blocks reentry when pacing is slow. Nevertheless, the rather common occurrences of ventricular

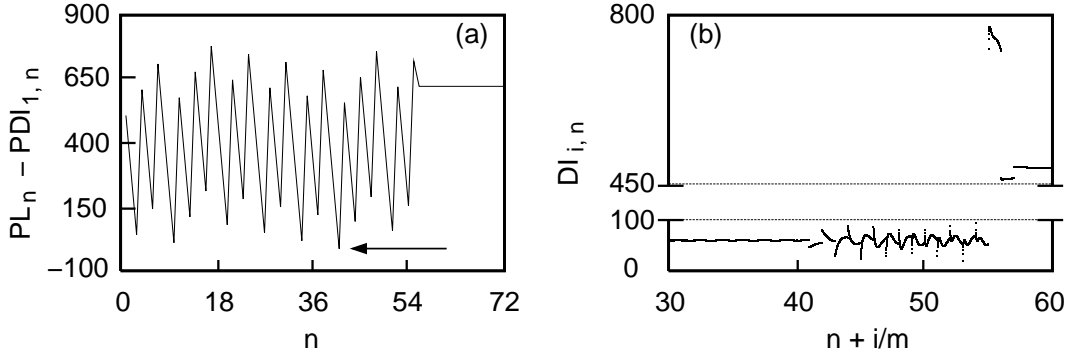


Figure 8: Results of Run 3.2. (a) Variations in $PL_n - PDI_{1,n}$ (see text). The negative value in Beat 41 (indicated by the arrow) corresponds to termination of reentry due to failure of TP. (b) DI values in Beats 30 through 60; note the phase resetting that occurs in Beat 41 and changes the reentrant circulation pattern from convergent to oscillatory in this T-bistable case.

tachycardia at low pacing rates in patients [58] motivate us to study this important special case in the context of a heterogeneous loop with a variable-rate pacer.

Suppose that the loop consists of two patches of cells. Patch 1 consists of cells 1 through j and Patch 2 contains cells $j + 1$ and beyond where of course, j is a positive integer less than m , the total number of cells. The cells in Patch 1 may have different APD and/or CT restitution parameters than those in Patch 2. For simulations, we also assume that the pacer has a variable-rate within the aforementioned nominal sinus range. Assume that the pacer’s oscillation period varies in a sinusoidal fashion:

$$B(k) = B_0 + B_1 \cos\left(\frac{2\pi k}{w}\right).$$

This beat pattern may represent an idealization (without random effects) of a single cycle of a complex, multi-pattern stretch of pacer beats. More complex variations may be considered in later studies if needed.

The number w is the period of a full cycle of variable-rate oscillations, which we refer to as a *full pacing cycle* (FPC). The halfway point of the FPC, or the “bottom of the FPC well” occurs at $k = w/2$; at this point, the pacer oscillates with minimum period (fastest beat rate). On the other hand, when $k = 0$ or $k = w$ the pacer has its largest oscillation period (slowest beat rate). The number B_1 is the FPC “amplitude” since it modulates the pacer’s oscillation period within the FPC. If $B_1 = 0$ then the period is a fixed B_0 as in the preceding case-studies.

Run 4.1. We fix the APD and CT parameters for Patch 2 to be the same as those used in Case-study 1. Patch 1 APD and CT have the same parameters as Patch 2 except for the following:

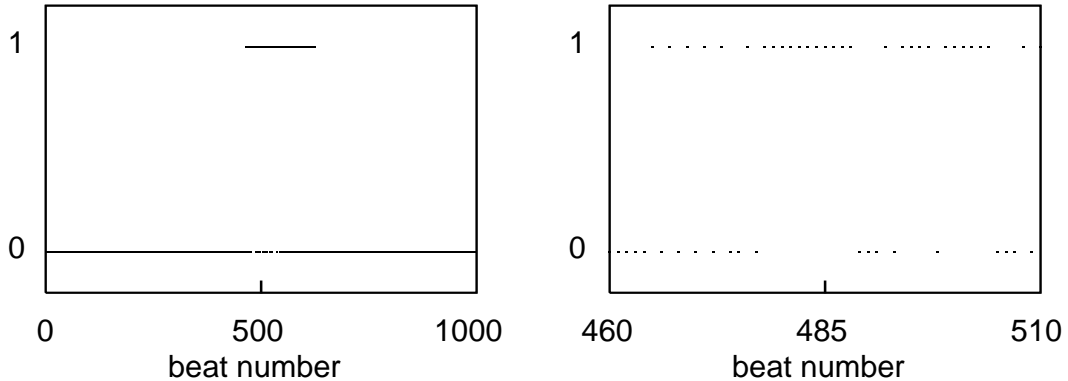


Figure 9: Schematic diagram of mode changes in Run 4.2. Beats in the reentry mode are listed with value 1 and those in the paced mode are given the value 0.

4 Further details of the model.

In this section we present additional supporting details about the model.

4.1 Remarks concerning the APD restitution function.

4.1.1 Memory and latency.

Experimental measurements and other studies reveal the difficulty of fitting a single curve to the data, particularly at the lower end of the DI scale. To address this and related issues, refinements have been considered in the forms of memory and latency. Beat to beat memory has been studied in [13, 19, 21, 23, 28, 46, 56] and has been modeled in a number of ways. In many cases, modeling memory can be accomplished by using DI values from several earlier stimulations. Latency (roughly a brief period between the arrival of a pulse and the firing of the cell) has also been expressed as a restitution function of DI [12, 13]. If this effect is added to APD we obtain a composite restitution function that may no longer be monotonic for small DI values. For simplicity, we ignore both memory and latency in this paper; however, they can (and need to) be included in the model for greater refinement in future studies.

4.1.2 Standard vs. dynamic protocols.

The APD restitution function may be measured experimentally using two different pacing protocols: Dynamic or standard (S1-S2) [29, 32]. These protocols generally produce APD curves that are shifted or have different slopes. For a discussion of this issue regarding the APD restitution that we use in this paper see [33]. The fit in (1) is to the dynamic restitution data in [33].

4.1.3 Remodeling.

The APD values (and thus the restitution function) may be affected by the steady fast pacing of the ventricles [34] or of the atria [39]. The implied shift in the APD restitution can have a significant effect on the SITR patterns in certain borderline cases. For simplicity we do not consider such effects in this paper; however, a suitable modification of the APD restitution function that incorporates explicit time dependence can accommodate dynamically-induced shifts.

4.1.4 APD non-monotonicity and spatio-temporal chaos.

Experimental evidence is offered in [53] that the APD restitution curve may be non-monotonic for small DI values. Working with a APD restitution curve having a single local minimum at low DI, the same study demonstrates the occurrence of spatial bifurcations along the length of a periodically paced fiber of cardiac tissue. Although not involving a loop structure, the work in [53] uses restitution functions in a discrete model. A localized form of non-monotonicity (like a bump or dent) in APD may occur at any DI value and has interesting consequences for additional complexity in reentry mode. In [48] where a continuous model of the loop as a cable is used, this type of non-monotonicity is shown to be responsible for the appearance of spatio-temporal chaos in APD and other key variables over the length of the loop. The occurrence of spatio-temporal chaos on the loop may raise the level of unpredictability in SITR if the amplitudes of oscillations in DI are large enough to let the wavefront reach its tail (thus causing a threshold failure).

4.2 Restitutions of ionic currents and conduction block.

Various anatomical and functional mechanisms for UB in a loop are discussed in the model study [49]. These mechanisms include a properly timed premature stimulus delivered to a suitable location in the loop, inhomogeneities in the degree of cellular uncoupling and gap junction resistance, in membrane excitability and in fiber cross sectional area. The discussion in [49] points to time, space and voltage “windows of vulnerability” for the occurrence of unidirectional block and initiation of reentry. Of these, the time window is seen to be the easiest to measure and its value is related to the space and voltage windows via standard mathematical formulas.

Each cell requires a certain amount of depolarizing current to fire an action potential. This *activation threshold* can be represented by a restitution function [27] or equivalently, the strength-interval curve [13] shifted to the left so that the origin represents the end of the ERP. In Figure 10 this curve is shown as a decreasing restitution function I_a .

In principle, at any time following the end of the ERP a sufficiently large current will be able to elicit an action potential. However, in the absence of external electrical shocks, there is a limited amount of current I_g available to depolarize the next cell. If a restitution of I_g is given then the intersection point of I_a and I_g is the *DI* threshold or cut-off value DI^* in the sense that if $DI > DI^*$ then action potential is fired and propagation occurs. The time interval DI^* is similar in nature to

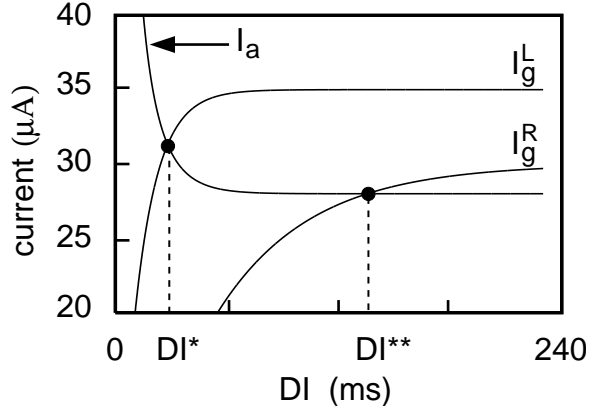


Figure 10: Activation and generated currents restitution curves illustrating the definition of DI^* and DI^{**} . In this figure, $I_a = I_a^L = I_a^R$ (see text).

the chronaxie [47] although the definition of DI^* requires another restitution curve in addition to I_a . A monotonically increasing restitution function for I_g might be appropriate; see Figure 10.

For our purposes here we do not need explicit formulas for either I_a or I_g . The value DI^* may be chosen arbitrarily or estimated experimentally without reference to its potential sources. Values as high as 160 ms were used in [26]. In human cases the value of DI^* in vivo is likely to be in a much smaller range. We use the conservatively small value of about 15 ms in this study.

An analog of the time window in [49] can be defined here using the restitution functions I_a and I_g . We define two sets of currents restitution functions for Cell 1 corresponding to the two possible directions in the loop: I_a^L, I_a^R and I_g^L, I_g^R for the “left” and the “right” directions. The asymmetry creates a *UB window* in Cell 1 as follows: Let $I_a^R \geq I_a^L$ and $I_g^R \leq I_g^L$ with at least one of these inequalities strict. Let DI^* be the (unique) intersection point of I_a^L and I_g^L and let DI^{**} to be the intersection point of I_a^R and I_g^R . Then $DI^* < DI^{**}$ and the interval between these two values is where the UB occurs. For if $DI_{1,n}$ represents the DI of Cell 1 in a cycle or beat n , then the conditions

$$DI^* < DI_{1,n} < DI^{**}$$

imply that propagation is possible in one direction because the threshold marked by DI^* is crossed but it is inhibited in the other direction where the DI^{**} threshold is not crossed.

We emphasize that the unidirectional block as defined here is functional and may not occur even if the UB window exists (for anatomical or functional reasons). If the number $DI_{1,n}$ does not enter the the UB window (i.e. the interval from DI^* to DI^{**}) in a particular beat n then the UB does not materialize. This option adds another mode to the loop-pacer system, namely the BDC mode mentioned previously. In addition to TC and TP, the following threshold is associated with the BDC mode:

TUB: $DI_{1,n-1} < DI^{**}$ with beat $n - 1$ in the paced mode.

This inequality defines the *UB threshold* to ensure that Cell 1 conducts unidirectionally. If beat $n - 1$ is in reentry mode then conduction in beat n is automatically unidirectional whether TUB holds or not, because the pulse is transmitted from a still active Cell m . To limit the variety of cases to consider, we assume in this paper that DI^{**} is so large that the unidirectional block is always present in Cell 1 (permanent UB) so TUB always holds.

5 Summary and discussion.

In the preceding sections, we developed an interactive loop-pacer threshold model that is a part of a familiar cardiac anomaly. Using experimental data on restitution parameters from the existing literature for action potential duration and conduction time, we obtained various conditions and parameter values that would cause irregular patterns of spontaneous initiations and terminations of reentry.

A major cause of unpredictable behavior is threshold bistability where one stable regime causes a failure of the circulation threshold TC and another does not. In this situation the initiation and termination of reentry depends on the location of the DI state vector in the m -dimensional state space, where the nonlinearity in propagation equations makes it difficult to track the state vector. Thus, it is quite difficult to forecast the long-term behavior of an evolving SITR pattern for a T-bistable loop. Another potential source of unpredictability is the interference by the pacer. If reentry occurs, then the pacer and the reentrant circuit are thrown out of phase so a phase resetting pacer pulse may unexpectedly end the reentrant circulation.

A number of prior studies of a different nature from ours also find complex SITR patterns in simple settings, such as in sheets [3, 25], loops [44] and aggregates [35] of animal cardiac tissue. In [3] and [25] complex patterns in monolayers of growing cell cultures are linked to changing densities and to local inhomogeneities, respectively. In [35] bursting beat patterns are studied in cell aggregates under external pacing. Closer to the subject matter of this paper, in [44] a ring-shaped lab preparation is considered with two localized pacemakers. Threshold relations for handling the pacers in this loop appear in the mathematical discussion. In a different class of studies, namely, the modulated parasystole, a permanent ectopic rhythm coexists with the sinus or another competing rhythm. In such relatively simple systems, complex beat patterns arise that are highly sensitive to parameter changes [23, 28, 43]. Like the TP threshold in our model, a mathematical relation with a discontinuity is responsible for the complexity of temporal patterns in parasystole; see [23, 43].

We omitted many features from our discussion here that one might include in an enhanced version of this model. For example, UB may be treated functionally by refining the UB time window and considering bidirectional propagation in the loop, as noted above. Other enhancements to this model might include adding memory and latency to the APD restitution function. The inclusion of memory is especially important in clarifying the dynamic significance of delayed responses (not

to mention improved fits to the APD restitution data). Additional directions for exploring the dynamics of the loop-pacer system include consideration of multiple exit/entry points into the loop that can affect reentry, a systematic approach to heterogeneity and also some theory to better model the time lag δ_n that influences the loop-pacer interactions. A somewhat different direction that may be explored would be to incorporate a programmed shock routine to artificially end long bursts of fast, reentrant beats.

With some of the above enhancements the SITR patterns will likely become more complex and less predictable, though it is also possible that some of these enhancements (e.g. memory) can have a moderating effect. Understanding the precise mechanisms that generate such complex SITR patterns may in turn offer new insights into the nature and causes of long-term temporal patterns of tachyarrhythmia occurrences.

REFERENCES

- [1] Anastasiou-Nana, M.I., R.L. Menlove, J.N. Nanas and J.L. Anderson, *Changes in spontaneous variability of ventricular ectopic activity as a function of time in patients with chronic arrhythmias*, *Circulation*, 78 (1988), 286-295.
- [2] Banville, I. and R.A. Gray, *Effects of action potential duration and conduction velocity restitution on alternans and the stability of arrhythmias*, *J. Cardiovascular Electrophysiol.*, 13 (2002), 1141-1149.
- [3] Bub, G., K. Tateno, A. Shrier and L. Glass, *Spontaneous initiation and termination of complex rhythms in cardiac cell culture*, *J. Cardiovascular Electrophysiol.*, 14 (2003), S229-S236.
- [4] Cain, J.W. *Criterion for stable reentry in a ring of cardiac tissue*, *J. Math. Biology*, 55 (2007), 433-448.
- [5] Cain, J.W. and D.G. Schaeffer, *Two-term asymptotic approximation of a cardiac restitution curve*, *SIAM Rev.*, 48 (2006), 537-546.
- [6] Cain, J.W., E.G. Tolkacheva, D.G. Schaeffer and D.J. Gauthier, *Rate-dependent propagation of cardiac action potentials in a one-dimensional fiber*, *Phys. Rev. E*, 70 (2004), 061906.
- [7] Cao, J-M., Z. Qu, Y-H. Kim, T-J. Wu, A. Garfinkel, J.N. Weiss, H.S. Karagueuzian and P-S. Chen, *Spatiotemporal heterogeneity in the induction of ventricular fibrillation by rapid pacing: Importance of cardiac restitution properties*, *Circ. Research*, 84 (1999), 1318-1331.
- [8] Chen, X., F.H. Fenton and R.A. Gray, *Head-tail interactions in numerical simulations of reentry in a ring of cardiac tissue*, *Heart Rhythm*, 2 (2005), 851-859.
- [9] S.S. Cheng, *Partial Difference Equations*, CRC Press, Boca Raton, 2003.
- [10] Cherry, E.M. and F.H. Fenton, *Suppression of alternans and conduction blocks despite steep APD restitution: Electrotonic, memory, and conduction velocity restitution effects*, *Am. J. Physiol.* 286 (2004), H2332-H2341.
- [11] Cytrynbaum, E. and J.P. Keener, *Stability conditions for the traveling pulse: Modifying the restitution hypothesis*, *Chaos*, 12 (2002), 788-799.

- [12] Derksen, R., H.V.M. van Rijen, R. Wilders, S. Tasseron, R.N.W. Hauer, W.L.C. Rutten and J.M.T. de Bakker, *Tissue discontinuities affect conduction velocity restitution: A mechanism by which structural barriers may promote wave break*, *Circulation*, 108 (2003), 882-888.
- [13] Chialvo, D.R., D.C. Michaels and J. Jalife, *Supernormal excitability as a mechanism of chaotic dynamics of activation in cardiac Purkinje fibers*, *Circ. Research*, 66 (1990), 525-545.
- [14] Courtemanche, M., L. Glass and J.P. Keener, *Instabilities of a propagating pulse in a ring of excitable media*, *Phys. Rev. Lett.*, 70 (1993), 2182-2185.
- [15] Courtemanche, M., J.P. Keener and L. Glass, *A delay equation representation of pulse circulation on a ring in excitable media*, *SIAM J. Appl. Math.*, 56 (1996), 119-142.
- [16] Courtemanche, M. and A. Vinet, *Reentry in excitable media*, in: A. Beuter, L. Glass, M.C. Mackey and M.S. Titcombe (Ed.s), *Nonlinear Dynamics in Physiology and Medicine*, Chapter 7, Springer, New York, 2003.
- [17] Elaydi, S.N. *An Introduction to Difference Equations*, (2nd ed) Springer, New York, 1999.
- [18] Fox, J.J., E. Bodenschatz and R.F. Gilmour, *Period-doubling instability and memory in cardiac tissue*, *Phys. Rev. Lett.*, 89 (2002), 138101(04).
- [19] Fox, J.J., R.F. Gilmour and E. Bodenschatz, *Conduction block in one-dimensional heart fibers*, *Phys. Rev. Lett.*, 89 (2002), 198101(04).
- [20] Frame, L.H. and M.B. Simson, *Oscillations of conduction, action potential duration and refractoriness: A mechanism for spontaneous termination of reentrant tachycardias*, *Circulation*, 78 (1988), 2182-2185.
- [21] Gilmour, R.F., M.A. Watanabe and N.F. Otani, *Restitution properties and dynamics of reentry*, In: *Cardiac Electrophysiology: From Cell to Bedside*, 3rd ed., W.B. Saunders, London, 1999, 378-385.
- [22] Girouard, S.D., J.M. Pastore, K.R. Laurita, K.W. Gregory and D.S. Rosenbaum, *Optical mapping in a new guinea pig model of ventricular tachycardia reveals mechanisms for multiple wavelengths in a single reentrant circuit*, *Circulation*, 93 (1996), 603-613.
- [23] Glass, L., A.L. Goldberger, M. Courtemanche and A. Shrier, *Nonlinear dynamics, chaos and complex cardiac arrhythmias*, *Proc. R. Soc. Lond. A* 413 (1987), 9-26.
- [24] Hall, G.M., S. Bahar and D.J. Gauthier, *Prevalence of rate-dependent behaviors in cardiac muscle*, *Phys. Rev. Lett.*, 82 (1999), 2995-2998.
- [25] Hwang, S-M., T.Y. Kim and K.J. Lee, *Complex-periodic spiral waves in confluent cardiac cell cultures induced by localized inhomogeneities*, *Proc. Nat. Acad. Sci. USA*, 102 (2005), 10363-10368.
- [26] Ito, H. and L. Glass, *Theory of reentrant excitation in a ring of cardiac tissue*, *Physica D*, 56 (1992), 84-106.
- [27] Jack, J.J., D. Noble and R.W. Tsien, *Electric Current Flow in Excitable Cells*, Clarendon Press, Oxford, 1975.
- [28] Jalife, J., C. Antzelevich and G.K. Moe, *The case for modulated parasystole*, *Pace*, 5 (1982), 911-926.

- [29] Kalb, S.S., H.M. Dobrovolny, E.G. Tolkacheva, S.F. Idriss, W. Krassowska and D.J. Gauthier, *The restitution portrait: A new method for investigating rate-dependent restitution*, J. Cardiovascular Electrophysiol., 15 (2004), 698-709.
- [30] Keener, J.P. *Arrhythmias by dimension*, In: *An Introduction to Mathematical Modeling in Physiology, Cell Biology and Immunology*, J. Sneyd (Ed.), 57-81, American Mathematical Society, 2002.
- [31] Kocic, V.L. and G. Ladas, *Global Behavior of Nonlinear Difference Equations of Higher Order with Applications*, Kluwer, Dordrecht, 1993.
- [32] Koller, M.L., M.L. Riccio and R.F. Gilmour, *Dynamic restitution of action potential duration during electrical alternans and ventricular fibrillation*, Am. J. Physiol. 275 (1998), H1635-H1642.
- [33] Koller, M.L., S.K.G. Maier, A.R. Gelzer, W.R. Bauer, M. Meesman and R.F. Gilmour, *Altered dynamics of action potential restitution and alternans in humans with structural heart disease*, Circulation, 112 (2005), 1542-1548.
- [34] Krebs, M.E., J.M. Szwed, T. Shinn, W.M. Miles and D.P. Zipes, *Short-term rapid ventricular pacing prolongs ventricular refractoriness in patients*, J. Cardiovascular Electrophysiol., 9 (1998), 1036-1042.
- [35] Kunysz, A.M., A. Shrier and L. Glass, *Bursting behavior during fixed-delay stimulation of spontaneously beating chick heart cell aggregates*, Am. J. Physiol. 273 (1997), C331-C346.
- [36] Lampert, R., L. Rosenfeld, W. Batsford, F. Lee and C. McPherson, *Circadian variation of sustained ventricular tachycardia in patients with coronary artery disease and implantable cardioverter defibrillators*, Circulation, 90 (1994), 241-247.
- [37] Liebovitch, L.S., A.T. Todorov, M. Zochowski, D. Scheurle, L. Colgin, M.A. Wood, K.A. Ellenbogen, J.M. Herre and R.C. Bernstein, *Nonlinear properties of cardiac rhythm abnormalities*, Phys. Rev. E, 59 (1999), 3312-3319.
- [38] Lown, B. *Sudden cardiac death: The major challenge confronting contemporary cardiology*, Am. J. Cardiol., 43 (1979), 313-328.
- [39] Manios, E.G., E.M. Kallergis, E.M. Kanoupakis, H.E. Mavrakis, H.K. Mouloudi, N.K. Klapsinos and P.E. Vardas, *Effects of successful cardioversion of persistent atrial fibrillation on right ventricular refractoriness and repolarization*, Europace, 7 (2005), 34-39.
- [40] Mickens, R. *Difference Equations: Theory and Applications* (2nd ed), CRC Press, Boca Raton, 1991.
- [41] Mines, G.R. *On dynamic equilibrium in the heart*, J. Physiol. (London), 46 (1913), 349-383.
- [42] Mitchell, C.C. and D.G. Schaeffer, *A two-current model for the dynamics of cardiac membrane*, Bull. Math. Biology, 65 (2003), 767-793.
- [43] Moe, G.K., J. Jalife, W.J. Mueller and B. Moe, *A mathematical model of parasystole and its application to clinical arrhythmias*, Circulation, 56 (1977), 968-979.
- [44] Nagai, Y., H. Gonzalez, A. Shrier and L. Glass, *Paroxysmal starting and stopping of circulating waves in excitable media*, Phys. Rev. Lett., 18 (2000), 184248(4).

- [45] Nolasco, J.B. and R.W. Dahlen, *A graphic method for the study of alternation in cardiac action potentials*, J. Appl. Physiol., 25 (1968), 191-196.
- [46] Otani, N.F. and R.F. Gilmour, *Memory models for the electrical properties of local cardiac systems*, J. Theor. Biol., 187 (1997), 409-436.
- [47] Plonsey, P. and R.C. Barr, *Bioelectricity: A Quantitative Approach* (2nd ed.), Kluwer Academic/Plenum Publ., NY, 2000.
- [48] Qu, Z., J.N. Weiss and A. Garfinkel, *Spatiotemporal chaos in a simulated ring of cardiac cells*, Phys. Rev. Lett., 78 (1997), 1387-1390.
- [49] Quan, W. and Y. Rudy, *Unidirectional block and reentry of cardiac excitation: A model study*, Circ. Research, 66 (1990), 367-382.
- [50] Sedaghat, H., C.M. Kent and M.A. Wood, *Criteria for the convergence, oscillation and bistability of pulse circulation in a ring of excitable media*, SIAM J. Appl. Math., 66 (2005), 573-590.
- [51] Sedaghat, H. *Nonlinear Difference Equations: Theory with Applications to Social Science Models*, Kluwer Academic, Dordrecht, 2003.
- [52] Stein, K.M., J.S. Borer, C. Hochreiter, and P. Kligfield, *Fractal clustering of ventricular ectopy and sudden death in mitral regurgitation*, J. Electrocardiol., (suppl) 25 (1992), 178-181.
- [53] Stubna, M.D., R.H. Rand and R.F. Gilmour, *Analysis of a nonlinear partial difference equation, and its application to cardiac dynamics*, J. Difference Equations and Appl., 8 (2002), 1147-1169.
- [54] Ten Tusscher, K.H.W.J., O. Bernus, R. Hren and A.V. Panfilov, *Comparison of electrophysiological models for human ventricular cells and tissues*, Prog. Biophys. Molecular Biology, 90 (2006), 326-345.
- [55] Vinet, A. *Quasiperiodic circus movement in a loop model of cardiac tissue: Multistability and low dimensional equivalence*, Ann. Biomed. Eng., 28 (2000), 704-720.
- [56] Watanabe, M.A., F.H. Fenton, S.J. Evans, H.M. Hastings and A. Karma, *Mechanisms for discordant alternans*, J. Cardiovascular Electrophysiol., 12 (2001), 196-206.
- [57] Watanabe, M.A. and M.L. Koller, *Mathematical analysis of dynamics of cardiac memory and accommodation: Theory and experiment*, Am. J. Physiol., 282 (2002), H1534-H1547.
- [58] Winkle, R.A., D.C. Derrington, J.S. Schroeder, *Characteristics of ventricular tachycardia in ambulatory patients*, Am. J. Cardiol., 39 (1977), 487-492.
- [59] Wood, M.A., P.M. Simpson, B.S. Stambler, J.M. Herre, R.C. Bernstein and K.A. Ellenbogen, *Long-term temporal patterns of ventricular tachyarrhythmias*, Circulation, 91 (1995), 2371-2377.
- [60] Wood, M.A., P.M. Simpson, W.B. London, B.S. Stambler, J.M. Herre, R.C. Bernstein, K.A. Ellenbogen, *Circadian patterns of ventricular tachycardia in patients with implantable cardioverter defibrillators*, J. Am. Coll. Cardiol., 25 (1995), 901-907.
- [61] Wood, M.A., P.M. Simpson, L.S. Liebovitch, A.T. Todorov and K.A. Ellenbogen, *Temporal patterns of ventricular tachyarrhythmias: Insights from the implantable cardioverter-defibrillator*,

in: S.B. Dunbar, K.A. Ellenbogen and A.E. Epstein (Ed.s), *Sudden Cardiac Death: Past, Present and Future*, Futura Pub. Co., Armonk, NY, 1997.